Characteristics and catalytic behavior of different platinum supported catalysts in the selective hydrogenation of soybean oil

Yuting Wang[1] · Xi Yang[1] · Yi Chen[1] · Shaoping Nie[1] ·
Mingyong Xie[1]

Abstract Platinum (Pt) catalysts supported on TiO_2, ZrO_2, activated carbon, and multi-walled carbon nanotubes were prepared by the wet impregnation method. The characterization of the obtained catalysts was performed with XRD, ICP-AES, TEM and N_2-adsorption. Their catalytic behavior during the selective hydrogenation of soybean oil was also studied. The results showed that compared with the commercial Raney Ni, all the platinum-catalysts exhibited better activity and lower selectivity towards *trans* isomer during the partial hydrogenation of soybean oil. Especially the Pt/ZrO_2 catalyst had the lowest selectivity towards the formation of *trans* C18:1 isomers and stearic acid. The results also showed that the metal loading had little impact on the hydrogenation activity and selectivity. Meanwhile, the acid value of hydrogenated oil over platinum-catalysts was less than 1.0 (KOH)/(mg/g). The hydrogenated oil over platinum-catalyst indicated good melting characteristics and solid fat content. These results demonstrated that Pt/ZrO_2 catalyst could be a good alternative of Raney Ni to reduce the formation of *trans* fatty acid and saturated fatty acid in hydrogenated soybean oil, and meanwhile ensure the physicochemical quality requirements of hydrogenated oils.

Keywords Platinum catalyst · Characterization · Hydrogenation of
soybean oil · Activity · *Cis–trans* selectivity · Physicochemical quality

---

✉ Yi Chen
   chenyi-417@163.com

[1]   State Key Laboratory of Food Science and Technology, Nanchang University, 235 Nanjing East Road, Nanchang 330047, Jiangxi, China

Introduction

The selective hydrogenation of edible oil is an important technology in the modification of fats and oils [1]. This conventional way can improve the thermal and oxidative stabilities and modify the melting characteristics and solid fat content of fats and oils, by reducing the concentration of unsaturated fatty acids and changing their physical and chemical properties [2–4]. It has been specifically applied in the production of shortenings, oleomargarines, bakery products and confectionary products with desirable characters [5, 6].

Most natural vegetable oils present C–C double bonds in *cis* configuration. During the hydrogenation process, in parallel with saturation of double bonds, geometric (*cis–trans*) and positional isomerization takes place [7]. The common industrial hydrogenation process is always carried out in batch slurry reactors at 150–225 °C and 3 bar pressure with finely dispersed Raney Ni catalyst [8, 9]. These commonly used hydrogenation conditions will lead to the formation of *trans* fatty acid (TFA) [10]. A possible association has been shown between the high intake of TFA and the risk of cardiovascular disease [11, 12]. Therefore, in order to minimize its health risk, new technologies are needed to reduce the overall content of TFA, and meanwhile meet the desired physicochemical quality requirements of oils. The catalytic interesterification of fully hydrogenated vegetable oils with conventional oils can yield *trans* free fat product but it still contains high levels of saturated fatty acid (SFA) [13]. However, research indicated a correlation between the intake of dietary SFA and high cholesterol levels and coronary heart diseases [14]. The selective catalytic hydrogenation is the process that allows selective conversion of unstable polyunsaturated fatty acids to more stable ones in a single step [13]. Despite the negative effects on health, the partial hydrogenation process is still widely used in the food industry [15]. In light of this, it is necessary to search for alternatives that improve the hydrogenation performance in order to reduce the TFA content [16].

Researchers have investigated the use of different supported metal catalysts to improve the activity and reduce the TFA level during hydrogenation, especially the noble metals such as platinum (Pt) and palladium (Pd) [17–19]. The noble metals dispersed on the solid supports demonstrated higher activity and in certain cases had a lower selectivity to TFA formation than commercial Ni. Compared with some other reported catalysts, the Pt has relatively higher activity and lower selectivity towards TFA formation via isomerization [17, 20, 21]. Besides the metal types, the solid support for the catalyst and its surface characteristics are also important factors contributing to the production of TFA and SFA during hydrogenation. This has been noted and studied by many researchers. Nohair and Especel [22] reported that the different supports had no influence on the selectivity and activity of the Pd catalyst during the hydrogenation process of sunflower oil. However, Fernández and Sánchez [23] showed that Pd catalyst supported on γ-Al$_2$O$_3$ with the highest dispersion and surface area was much more active than the others (α-Al$_2$O$_3$, ZSM-5 and MCM-22). Therefore, it is necessary to re-explore the effects of metal particle

size and the supports structure on the activity and selectivity of novel metal catalysts in the partial hydrogenation of vegetable oil.

Carbon materials like AC or multi-walled carbon nanotubes (MCNTs) are promising catalyst supports as they allow tuning catalytic properties and performance, due to their unique physical and chemical properties, such as defined pore shapes and sizes, large surface areas, excellent chemical stability and electronic binding energy [24–26]. However, there is no systematic investigation of the effects of these catalyst supports materials on activity and *cis–trans* selectivity of catalysts during oil hydrogenation.

In our previous work, Pt catalyst supported on ZrO_2, compared with Raney Ni, demonstrated a superior performance for partial hydrogenation of soybean oil. The objective of this study, based on our preliminary experimental results, is to examine the influence of metal particle size, supports characteristics and metal content on the activity and selectivity (toward *cis*-monoenes and saturated stearic acid) of Pt catalyst for soybean oil hydrogenation. Thus, ZrO_2, TiO_2, and other widely used supports including AC and MCNTs were selected as catalyst supported material in present study. A comparative evaluation of Pt catalysts and a commercial Raney Ni catalyst was carried out. In addition, the melting points and solid fat content (SFC), acid value were chosen to investigate the physical and chemical properties of hydrogenated oil over Pt/AC, Pt/MCNTs, Pt/ZrO_2, Pt/TiO_2 and Raney Ni catalysts.

Experimental

Materials and chemicals

Activated carbon (AC) was purchased from Shaowu Xinsen Chemical Industry Co. Ltd. (Fujian, China). The multi-walled carbon nanotubes (MCNTs) were purchased from Chengdu Organic Chemicals Co. Ltd (Chengdu, China). $TiCl_4$, and $ZrO(NO_3)_2$ were purchased from Xiya Reagent (Chendu, China). Hexachloroplatinic acid ($H_2PtCl_6 \cdot H_2O$, 99.9%) was purchased from Sigma (St. Louis, MO, USA). Raney Ni was obtained from Shangdong Jiahong Chemical Engineering Ltd. (Shangdong,China). Mixed standards GLC-463, methyl heneicosanoate (C21:0, FAME) and internal standard triheneicosanoin methyl ester (C21:0, TAG) were purchased from Nu-Chek Prep, Inc. (Elysian, MN, USA). Linoleic acid methyl ester isomer mix and linolenic acid methyl ester isomer mix bought from Supelco Inc. (Bellefonte, PA, USA). N-heptane of chromatographic grade was obtained from Fisher Scientific (Fair Lawn, NJ, USA). Potassium hydroxide, chloroform and methanol were of analytical grade. Soybean oil was bought from a local supermarket.

Preparation of catalysts

TiO_2 was obtained by the hydrolysis of $TiCl_4$ in solution. ZrO_2 was obtained by the hydrolysis of $ZrO(NO_3)_2$ aqueous solution of ammonia. According to the McArdle method [17], the Pt/AC (AC without activation or oxidation pretreatment), Pt/ZrO_2

and Pt/TiO$_2$ were prepared by wet impregnation with hexachloroplatinic acid as the precursor salt. The Pt/MCNTs catalyst was also prepared using the McArdle wet impregnation method with minor modifications. Before impregnation, the MCNTs support should be activated with the concentrated nitric acid by heating under reflux at 80 °C for 4 h, and was then washed with distilled water until neutral, followed by drying in an oven at 80 °C for 12 h. The required amount of activated MCNTs was dissolved in a mixture solution of 5 mL ethanol and 25 mL distilled water, and was then dispersed by ultrasonication for about 30 min. After stirring for a few minutes, it was heated at 80 °C for 30 min. Then an aqueous solution of hexachloroplatinic acid was added and the mixture was kept stirring for 15 min. Formaldehyde solution (35 mL) was then added as the reductant. Then the impregnated catalyst was reduced and dried following the McArdle method [17]. The concentration of the impregnating solution was counted to ensure a Pt loading of 2 wt% in the above catalysts. Finally, the catalysts were calcined in a furnace at 450 °C for 5 h, and then further reduced by hydrogen in the tubular furnace at 500 °C for 4 h.

Catalyst characterization

The phase and crystal structure of the catalysts were analyzed by powder X-ray diffraction (XRD) using a diffractometer (XRD Di System, Bede Company, Durham, United Kingdom) operating at 40 kV and 40 mA with Cu K$_\alpha$ radiation ($\lambda = 1.542$ Å). Scans were collected from the X-ray source angles 10°–80°.

The average platinum loadings on the support were analyzed by means of inductively coupled plasma-atomic emission spectroscopy (ICP-AES). The analysis was taken on an OPTIMA 5300DV ICP-AES spectrometer (Perkin-Elmer Corp., Norwalk, CT, USA) over a wavelength range between 165 and 780 nm and under an optical resolution less than 0.006 nm.

N$_2$ adsorption–desorption experiment were performed at the temperature of liquid nitrogen (-196 °C) by a Micrometrics ASAP-2020 V3.03 G instrument (Micromeritics Instrument Corporation, Norcross, GA, USA). The specific surface area measurement of the bare supports and obtained catalysts was calculated by the BET method. The pore volume and pore size distribution of the sample were generated from the N$_2$ adsorption isotherm using the Barrett–Joyner–Halenda theory. Before the adsorption analysis, each sample was degassed in vacuum for 6 h at 200 °C.

The morphology and microstructure of the supports and catalysts were detected by transmission electron microscope (TEM) method. The measurements were carried out on a TEM apparatus (JEM2010, JEOL, Tokyo, Japan) with an acceleration voltage of 200 kV and under a space resolution of 0.24 nm.

Hydrogenation of soybean oil

The test of these platinum-supported catalysts for the hydrogenation of soybean oil was carried out using GSA-1L reactor vessel (Jiayi Company, Weihai, China). The reactor was connected to a hydrogen source maintained at a constant pressure.

The hydrogenation conditions were selected to reproduce similar industrial operating conditions. Typically, 300 g of soybean oil and 150 mg catalyst were charged into the reactor vessel. Then the reactor vessel was purged with flowing nitrogen to guarantee an oxygen free atmosphere. When the temperature of the system increased gradually to 170 °C, hydrogen was then introduced into the reactor. This moment was referred to as the time "zero" of reaction. Meanwhile, the impeller was started to agitate the slurry at a stirring rate of 400 rpm. The hydrogen pressure was maintained constantly at 3 bar throughout the whole reaction. Oil samples were withdrawn every half hour from the reactor vessel and the entire reaction time was 4 h.

A traditional commercial Raney Ni catalyst was used as a reference. Conventional Raney Ni (fine-grained solid) composed mostly of nickel derived from a nickel-aluminum alloy in the proportion of 50:50 wt% (Ni:Al = 1:1).

The hydrogenation products were analyzed for their iodine value (IV) according to GB/T 5532-2008. The iodine value change of oil was used to calculated the activity of catalysts during hydrogenation.

Fatty acid composition analysis

For the analysis of fatty acid composition, following the method that we previously developed [27], the oil sample was converted into its fatty acid methyl esters (FAMEs) with potassium hydroxide–methanol prior to gas chromatography (GC) analysis. The GC analysis of the hydrogenated oil was taken on Agilent 6890 N GC instrument, which was connected to a flame ionization detector (FID) and an Agilent 7683B autosampler with a split/splitless injector. The separation of FAMEs was carried on a fused-silica capillary column CP Sil-88 (100 m × 0.25 mm id., 0.20 μm film thickness, Varian Inc.,USA). The detection of FAMEs was performed under the detail condition as we have published [28].

Mixed standards GLC-463, methyl heneicosanoate (C21:0, FAME), linoleic acid methyl ester isomer mix and linolenic acid methyl ester isomer mix were used as reference standards to identify individual FAME by their elution time. The amount of FAs was calculated bythe internal standard quantitative method. Triheneicosanoin methyl ester (C21:0, TAG) was used as the internal standard.

Physical and chemical properties analysis of hydrogenated oil

The acid value of the hydrogenated on the different catalysts oil was analyzed according to GB/T 5530-2005. The slide melting points of each sample were observed by SGW X-4 Microscopic melting point apparatus (Shanghai Precision & Scientific Instrument CO., LTD., Shanghai, China).

The solid fat content of the hydrogenated oil was measured by method of low resolution nuclear magnetic resonance using NMI20 Analyst (Shanghai Niumag Corporation, Shanghai, China). According to the AOCS Official Method Cd 16b-93, the samples were evaluated at 10, 15, 20, 25, 30, 35, 40, 45 and 50 °C. Each sample was kept at 0 °C for 60 min and then at each reading temperature for 30 min.

Results and discussion

Characterization of synthesized catalysts

After the activation procedure, the catalysts and supports were analyzed by XRD and some characteristic peaks of crystalline Pt could be observed, including plane (111), (200), (220) at 2θ of 39.78°, 46.26°, 67.48°. No characteristic diffractions of crystalline PtO_x could be detected in the spectra, indicating the uniform dispersion of the particles throughout the matrix of supports. Furthermore, for Pt/ZrO_2, the same characteristic peak positions and intensities for ZrO_2 were observed. These results indicated that the introduction of Pt particle into ZrO_2 did not change the crystal structure of the support here. According to the results of ICP-AES analysis, the actual metal loadings of Pt/TiO_2, Pt/ZrO_2, Pt/AC and Pt/MCNTs catalysts were 1.21, 1.79, 1.56 and 1.73 wt%.

The textural characterization of supports and platinum-supported catalysts were studied by analysis of nitrogen isotherms and the absorption data. Fig. S2 shows the nitrogen absorption–desorption isotherms of all supports and catalysts. The shape of the adsorption isotherms linear plot of AC, MCNTs were Type IV, while ZrO_2, TiO_2 were the Type V [29]. AC and MCNTs represented the Type IV which was the typical mesoporous materials with multi-layer absorption. Otherwise ZrO_2, TiO_2 represented Type V, which was associated with large inter molecule attraction effects. In addition, the hysteresis loop of AC seemed to be of type H_4 IUPAC classification, which represented the narrow slit-shaped pores associated with the layered structure of activated carbon. The hysteresis loop of MCNTs seemed to be of type H_3, the absorption of nitrogen at high pressure (0.5–0.9 P/P_0) was significantly increased compared to H_4. While the hysteresis loop of Pt/ZrO_2 and TiO_2 seemed to be the H_1, which was associated with the homogeneous pores model having an evident slip-shape pores. However, for TiO_2, the shape of adsorption isotherm was changed after impregnation. This might result from the agglomeration of TiO_2 particles, corresponding to the gradual appearance of the diffraction peak at 2θ of 77.4° in the XRD pattern.

The pore size distribution of the supports and catalysts obtained from the absorption data were summarized in Table 1. The Pt/AC, Pt/MCNTs, Pt/ZrO_2 and Pt/TiO_2 catalysts showed an average diameter of 2.71, 4.48, 16.16 and 16.47 nm. The mesoporous solids (AC and MCNTs) showed the main pore diameter of 2.54 and 4.95 nm. Both values were in agreement with the reported average pore diameter for these materials. In the cases of ZrO_2 and TiO_2, the pore diameter was 15.53 and 8.08 nm. Moreover, the corresponding pore diameters of the Pt/AC, Pt/MCNTs and Pt/ZrO_2 catalysts were very similar to that of the support, indicating only a slight modification of the textural characteristics of the support after impregnation. While for Pt/TiO_2, there was a slight decrease in pore size with impregnation. This was in consistent with our above results obtained from the nitrogen absorption–desorption isotherms.

As shown in Fig. 1, larger Pt particles formed on the MCNTs catalyst (Fig. 1c) with average diameter of 4.0 ± 1.5 nm, whereas smaller Pt particles tended to form

Table 1 Textural properties of supports and synthesized catalysts

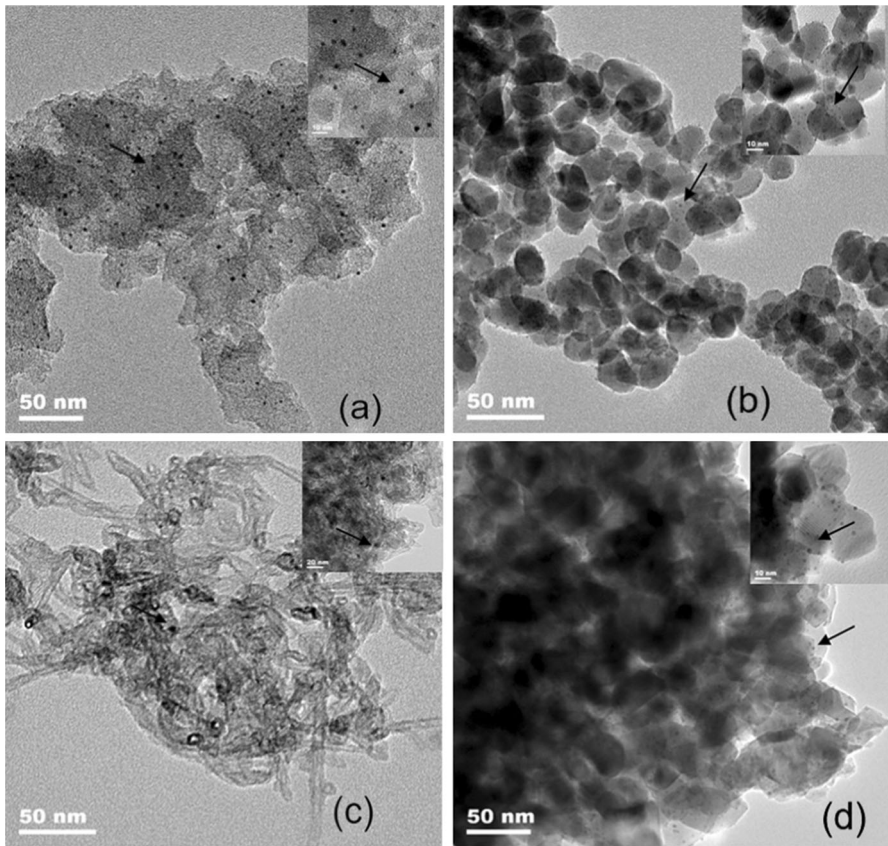| Catalyst name	Specific surface area (m^2g^{-1})	Pore volume (cm^3g^{-1})	Pore diameter (nm)	Particle size TEM (nm)
AC	1622.51	1.03	2.54	–
1.56% Pt/AC	1755.86	1.19	2.71	2.5 ± 0.5
ZrO_2	26.32	0.10	15.53	–
1.79% Pt/ZrO_2	32.88	0.13	16.16	1 ± 0.25
MCNTs	454.92	0.56	4.95	–
1.73% Pt/MCNTs	412.12	0.46	4.48	4.0 ± 1.5
TiO_2	79.94	0.16	8.08	–
1.21% Pt/TiO_2	19.37	0.08	16.47	2.5 ± 0.25

Fig. 1 TEM images of synthesized catalysts: **a** Pt/AC, **b** Pt/ZrO_2, **c** Pt/MCNTs, **d** Pt/TiO_2. The *black blot* which the *arrow* highlighted was the Pt particles on the support materials

on the AC, TiO_2 and ZrO_2 catalysts (Fig. 1a, b and d) with average diameter from 2.5 ± 0.50, 2.5 ± 0.25 to 1.0 ± 0.25 nm.

When comparing morphologies of these catalysts, the Pt/AC and Pt/ZrO_2 catalysts showed fractal structures with spherical building units (Figs. 1a and 1b), which were consistent with good dispersibility of the synthesized catalysts. In contrast, the Pt/TiO_2 catalyst did not show an open structure (Fig. 1d) that corresponded to the significant agglomeration phenomenon. For the Pt/MCNTs catalyst, a typical TEM image of MCNTs was shown in Fig. 1a, from which it can be seen that the spherical Pt particles, the dark spots trapped inside the MCNTs were quite uniform and distributed homogeneously.

Table 1 also summarizes the specific surface area of each sample. It clearly showed that the catalysts with the lower BET surface area tended to have a larger average pore diameter. This demonstrated that the high surface areas of catalysts favored the high dispersion of Pt species, thus small platinum particles were formed on the support. It could be concluded that Pt species were well dispersed on the Pt/AC, Pt/MCNTs and Pt/ZrO_2 catalysts, but not well on the Pt/TiO_2. The relatively homogeneous dispersion could be attributed to the relatively strong metal/support interaction between the metal salt precursor and the supports [30].

The activity and selectivity of catalysts

The activity of each catalyst was assessed by measuring the fall in iodine value (IV) during hydrogenation, with which the C=C conversion [31] could be obtained according to the following equation:

$$C=C \text{ conversion} (\%) = \frac{(IV_0 - IV_f)100}{IV_0},$$

Here IV_0 is the initial IV of the soybean oil, IV_f is the corresponding iodine value of the hydrogenated oil at each testing time. Fig. S3a shows the changes of IV of the oil with different catalysts over 4 h of hydrogenation. The 1.79 wt% Pt/ZrO_2 catalyst showed the highest activity with the reduction of IV from 140 to 22.27 in 4 h, which was equal to a C=C conversion of 84.1%. However, it should be noted that this catalyst also contained the highest amount of impregnated metal content. The 1.56 wt% Pt/AC catalyst had a little better activity than the 1.73 wt% Pt/MCNTs catalyst because the C=C conversion was 56.2% for the Pt/AC catalyst, compared to a conversion of 49.3% for the Pt/MCNTs catalyst. Among all these Pt catalysts, the lowest activity was observed for the 1.21 wt% Pt/TiO_2 catalyst, which reached a conversion of 38.1%. Nevertheless, it was still higher than that of the Raney Ni catalyst. The results suggested that the nature of the support had a great influence on catalyst activity during the hydrogenation of soybean oil under the selected operating conditions. This is a common phenomenon and was reported in the literature [23]. The different supported Pt catalysts have variable surface morphology (dispersion, particle sizes and surface area), which might give the rise of the difference in activity. As Table 1 shows, the Pt/ZrO_2 presented smaller particle sizes than the other catalysts in this investigation. Besides, Pt particles were well dispersed on the

Pt/ZrO$_2$. Taken together, it might contribute to the high activity of Pt/ZrO$_2$ catalyst. Meanwhile, the differences in activity may not only result from the various supports but also from the slight difference in metal contents. As the results presented in Fig. S3a, there seemed to be a correlation between the fall in IV and metal contents for the catalyst tested. Thus, a further study was conducted to demonstrate the influence of the metal contents on the catalysts activity.

Three different Pt/ZrO$_2$ catalysts with the platinum loadings of 2, 5 and 8 wt% were compared. According to the results of ICP-AES tests, the actual metal loadings of these catalysts were 1.81, 4.93 and 7.98 wt% of Pt/ZrO$_2$. Fig. S3b presents the fall in IV over the first hour of hydrogenation and its relationship with the metal loading. The 5% Pt/ZrO$_2$ presented lower hydrogenation activity, very similar to the 8% Pt/ZrO$_2$, and slightly higher activity was observed for the 2% Pt/ZrO$_2$ (the lowest Pt metal loading). Moreover, the linoleic acid (C18:2) conversion rates after 4 h of the hydrogenation reaction for these three catalysts were also similar (98.84, 97.51 and 96.71%). The above results indicated that the metal loading effect had a little impact on the hydrogenation activity from 2 to 8 wt% Pt. This was a little similar with the phenomena reported in literature that the activity improved with the increased amount of supported Pt, while levelled off somewhat at content above 2 wt% Pt [17]. These results may be explained by the fact that the reaction rate of hydrogenation was controlled by the limited level of H$_2$ dissolved in the oil rather than the metal loading of the catalyst. Therefore, the metal loading has a weaker influence on the activity than the nature of the support.

In order to make a clear comparison between the selectivity of different supported catalysts, it is better to compare them at a fixed activity level. Edible oils are often industrially hydrogenated to an IV of 70. Therefore, in this study, the characteristics of the catalysts were compared at an IV of 70. Fig. 2a presents the change in the oil fatty acids composition for the hydrogenation carried out by Pt/AC catalyst. High activity was shown for the Pt/AC catalyst reaching an IV equal to 78 after 3 h. The content of *cis*-linoleic acid (C18:2) steadily decreased from the initial value of 59.37 to 2.98%, whereas the content of *trans*-oleic acid (C18:1) increased over the course of reaction from 0 to 29.67%. *Trans*-C18:2 showed a different behavior with an increase up to 6.99% (30 min) followed by a decrease to 2.90% due to the conversion to the *trans*-oleic acid (C18:1) and the stearic acid (C18:0). There was a corresponding increase in the formation of *cis*-oleate (C18:1) for up to 2.5 h hydrogenation and after that a gradual decrease was observed. The content of stearic acid (C18:0) remained at less than 10% for up to 70 min, and then rapidly increased to a final value of 28.86%. The linolenic acid (C18:3) was not considered for its low concentration.

The evolution of reactants and products with hydrogenation time for the Pt/ZrO$_2$, Pt/MCNTs and Pt/TiO$_2$ catalysts were also determined. As shown in Figs. 2b, 2c and 2d, a similar overall reaction pathway was observed, but the magnitudes for each reaction step were different. Similar activity of Pt/MCNTs and Pt/AC were followed from the IV trend and the conversion of linoleic acid (C18:2). The IV for Pt/MCNTs reached a final value of 71% (reaction extent: 49.3%). Similarly, the Pt/AC reached a final value of 61.31% (reaction extent: 56.2%). This can also be seen
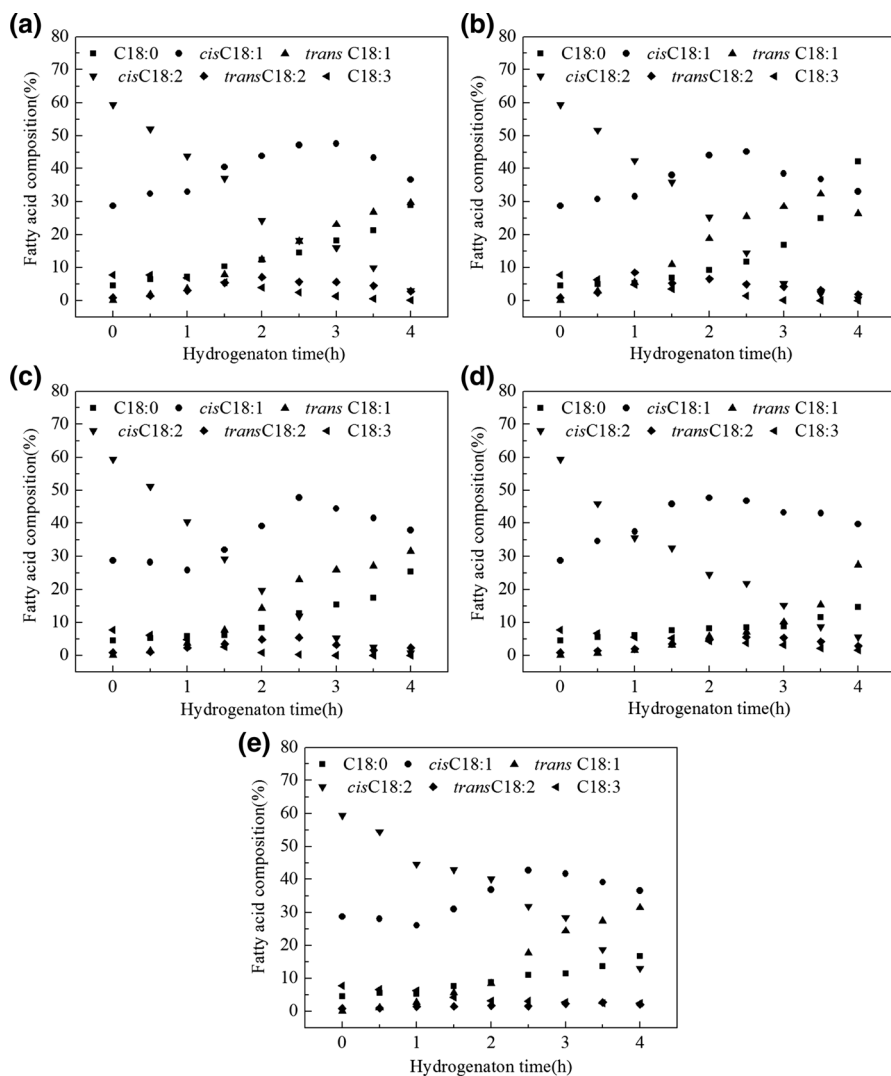
Fig. 2 The changes of fatty acid composition of hydrogenated oils over different catalysts during different hydrogenation processes (temperature 170 °C, pressure 3 bar, stirring rate 400 rpm), **a** Pt/AC, **b** Pt/ZrO$_2$, **c** Pt/MCNTs, **d** Pt/TiO$_2$, **e** Raney Ni

from Fig. 2c, which shows a steady drop in the C18:2 concentrations to the final value of 0.871% and a corresponding increase of the TFA content.

It was evident from these graphs that the Pt/ZrO$_2$ was the most active since the concentration of *cis*-linoleic acid (C18:2) decreased more rapidly (from 59.37 to 0.37%). Its high activity could also be confirmed from a rapid decrease in IV from 140 to 70 in less than 130 min. Once the linoleate (C18:2) was consumed, a steady increase in stearate (C18:0) formation was observed, finally forming a very high level of saturate acid (42.13%) as the *trans*- and *cis*- forms of C18:1 decreased. The

lowest activity was observed for the Pt/TiO$_2$ catalyst and this can be seen in the small and slow changes in its stearic acid content, as shown in Fig. 2d.

Nearly the same behavior was observed with Raney Ni catalyst (Fig. 2e). The *cis*-C18:2 was converted by hydrogenation and isomerization, and its level decreased during the reaction. The levels of *cis*-oleic acids concentrations increased, and then decreased as a result of their conversion to stearic acid, and possibly also to *trans*-monoenoic acids.

Thus as indicated above, the overall hydrogenation reaction might involve the consecutive saturation of *cis*-C18:2 to *cis*-C18:1 and its subsequent saturation to C18:0, as well as the parallel isomerization of *cis*-C18:2 to *trans*-C18:2 and *cis*-C18:1 to *trans*-C18:1. The reaction pathway could also involve the hydrogenation of *trans*-C18:2 to *cis*-C18:1 and *trans*-C18:1 to C18:0.

In all the cases, there was an increase in the concentration of stearic acid (C18:0) and a decrease in linoleic and linolenic acids (*cis*-C18:2 and *cis*-C18:3) due to the saturation of the double bonds. Compared with the Ni catalyst, a smaller amount of TFAs but more selective toward *cis*-C18:1 formation was produced with the Pt catalysts for the same IV reduction. Pt/ZrO$_2$ catalyst exhibited an activity obviously higher than that of the Ni catalyst and with the lowest production of SFA (11.78%) and *trans*-C18:1 (25.48%). While the Ni catalyst produced the highest amount of *trans*-C18:1 (31.42%) at an IV of 98.79, the Pt/AC and Pt/TiO$_2$ catalysts exhibited selectivity towards *trans*-C18:1 comparable to that of the Pt/ZrO$_2$ catalyst but with higher production of SFA (21.43 and 14.61%). Compared with some previous studies, Pt/ZrO$_2$ catalyst in this study had lower selectivity towards *trans*-C18:1 and stearic acids. McArdle et al. [17] showed in their study that all of the tested catalysts (1.45% Pd/ZrO$_2$, 1.36% Pt/ZrO$_2$, 0.74% Pd/Al$_2$O$_3$, 0.85% Pd/Al$_2$O$_3$, 1.7% Pd/Al$_2$O$_3$, 2.1% Pd/Al$_2$O$_3$, 3.86% Pd/Al$_2$O$_3$, 1.28% Pd/TiO$_2$, 1.98% Pt/TiO$_2$) produced more than 30% *trans*-C18:1 and relatively high level of stearic acid at an iodine value of 70. Besides, another literature reported that the 4.6% Pt/SiO$_2$ catalyst produced the highest level of *trans*-C18:1 (33%) and lowest level of stearate (14%) for the catalyst examined, while the 1.5% Pt/SiO$_2$ and 2.7% Pt/SiO$_2$ catalysts formed similar levels (26.4 and 27%) of *trans*-C18:1 and relatively higher amount (19.2 and 16.5%) of stearate, at an iodine value of 70 [32]. From the results, it is clear that the different supported catalyst showed different selectivity towards the *trans*- isomer and SFA. For both Pt/ZrO$_2$ and Pt/TiO$_2$ catalysts, the yields of SFA were lower than that of Ni, which might be attributable to the difference in the affinity of dienoic and monoenoic acids and their stronger adsorption on the dispersed Pt, thus favoring the formation of monoenoic acids rather than stearic acid. However, both Pt/MCNTs and Pt/AC catalysts, which exhibited greater pore volumes and smaller mean pore diameters than other catalysts, produced higher levels of SFA. These results suggested that the pore geometry of the support for Pt catalysts might also facilitate a higher hydrogenation of polyunsaturated TAGs. The presence of deeper pores in these two supported Pt catalysts may allow a longer residence time of unsaturated TAGs, thus promoting their hydrogenation. Several researchers reported the effects of the support, dispersion and particle size of the metal on the levels of TFA in the hydrogenated oils [22, 32]. They suggested that the smaller metal particles seemed to yield less TFA. In this study, it also showed

that the selectivity to *trans*-monoenoic acids and stearic acid was influenced by the Pt particle size. The Pt/ZrO$_2$ exhibited the smallest particles size and was less prone to form stearic acid and *trans*-monoenoic acids during hydrogenation process.

Table 2 summarizes the selectivity and isomerization index of each catalyst. S$_1$ is defined as the amount of monounsaturated fatty acids (C18:1) formed during the hydrogenation with respect to the amount of di-unsaturated fatty acids (C18:2) converted, and selectivity S$_2$ is defined as the amount of saturated fatty acids (C18:0) produced with respect to the amount of monosaturated fatty acids (C18:1) converted [22, 23]. SI (isomerization index) (11) is described as the proportion of double bonds isomerized to the *trans* configuration relative to those saturated with hydrogen. As shown in Table 2, Pt/ZrO$_2$ catalyst exhibited the highest S$_1$ among all these catalysts, followed by Pt/AC catalyst and the Ni catalyst, indicating that Pt/ZrO$_2$ catalyst was the most selective toward (*cis*)-C18:1 formation. On the other hand, the values of S$_2$ were 0.41 and 0.17 for Pt/AC and Pt/ZrO$_2$, indicating that the saturation of C18:1 to C18:0 was more pronounced for the Pt/AC catalyst and lowest for the Pt/ZrO$_2$ catalyst. Despite of the obviously increasing C18:0 in the hydrogenated products, the amount of C16:0 also increased during the hydrogenation process. The amounts of C16:0 in the hydrogenated oils were almost the same for the Pt/ZrO$_2$ and Pt/AC catalysts, 17.63 and 17.17%, respectively. While compared to the original soybean oil, the C16:0 were a lot higher for the Pt/TiO$_2$ and Ni catalysts. The values of isomerization index, SI, were 0.210 and 0.276 for Pt/ZrO$_2$ and Pt/MCNTs catalysts, compared to 0.476 for the Ni catalyst. The lower SI values of Pt catalysts indicate their lower isomerization activity for a given saturation activity, as seen by somewhat lower TFA production by these catalysts compared to the Ni catalyst.

Table 2 Comparison the characteristics of oil before and after hydrogenation (temperature 170 °C, pressure 3 bar, and stirring rate 400 rpm)

	Soybean oil	Partially hydrogenated oil				
		Pt/AC	Pt/ZrO$_2$	Pt/MCNTs	Pt/TiO$_2$	Raney Ni
Fatty acids (g/100 g oil)						
C16:0	13.84	17.17	17.63	14.70	25.50	22.52
C18:0	4.55	21.43	11.79	17.51	14.61	16.18
*trans*C18:1	0	26.77	25.48	27.04	27.41	31.42
*cis*C18:1	28.69	43.31	45.12	41.56	39.67	36.50
C18:2	60.23	14.37	20.63	4.08	8.45	15.06
C18:3	7.66	0.45	0.86	0	1.55	2.44
S$_1$[a]	–	0.90	1.06	0.72	0.74	0.87
S$_2$[b]	–	0.40	0.17	0.32	0.26	0.29
IV	140	78.04	67.50	72.6	86.65	98.79

[a] S$_1$ = (C18:1–C18:1$_0$)/(C18:2$_0$–C18:2)

[b] S$_2$ = (C18:0–C18:0$_0$)/(C18:1–C18:1$_0$)

Physical and chemical properties of hydrogenated oil

In this study, in order to compare the changes of physical and chemical properties of hydrogenated oil over different catalysts, the melting point and solid fat content were chosen to studied [33, 34]. Besides, the acid value (AC) was also used to describe their stabilities.

The melting points of hydrogenated oil over Pt/ZrO$_2$, Pt/AC, Pt/MCNTs, Pt/TiO$_2$ and Raney Ni catalysts were determined. The melting point plays a significant role in characterizing and developing fats [35]. Fig. S4 shows the melting characteristics of hydrogenated oil catalyzed over Pt/AC, Pt/ZrO$_2$,Pt/MCNTs, Pt/TiO$_2$ and Raney Ni. The results showed that hydrogenated oil obtained using Pt/AC, Pt/ZrO$_2$, Pt/MCNTs had a good melting point of 36.7, 32.8, 36.6 °C. While the melting points of the hydrogenated oil obtained over Pt/TiO$_2$ and Raney Ni were only 25.5 and 24.9 °C, respectively, after 4 h of reaction. This limits the application of hydrogenated fats. The difference in the melting characteristics of the hydrogenated oils is due to the different fatty acids profile. The TFAs have melting points higher than the corresponding *cis* fatty acids, but lower than the saturated acids. For example, oleic acid (*cis*-C18:1) melts at 16.3 °C, its *trans* isomer, *trans*-oleic acid (*trans*-C18:1), melts at 44 °C, and stearic acid (C18:0) melts at 72 °C. Therefore, the differences in the contents of stearic acid and *trans*-monoene led to the different melting characteristics of above hydrogenated fats.

Solid fat content (SFC) curve is useful for formulating and developing new fat products as it could give a good indication of overall behavior of oils and fats [36] The solids content of oils and fats is responsible for many physical and sensory properties, including appearance, spreadability, ease of packaging, plasticity, texture and organoleptic properties [37]. The solid–liquid proportion of hydrogenated oil was important to its consistency and melting, plasticity properties at a given temperature. SFC of hydrogenated oils was determined at different temperatures from 10 to 50 °C by the pulsed NMR [38] and presented in Fig. S5. As the results showed, the SFC profiles of all hydrogenated oil were significantly different from each other. The SFC values of hydrogenated oil over Pt/AC, Pt/ZrO$_2$ and Pt/MCNTs were relatively high while that of hydrogenated oil over Pt/TiO$_2$ and Raney Ni were lower. These were in harmony with the melting characteristics. It indicated that the SFC was found to be temperature dependent. Besides, the evolution of SFC value was related with both the fatty acid composition of each hydrogenated product.

According to the hygienic standard of edible oil, the AV for oleomargarine should be less than 1.0 (KOH)/(mg/g) and for the vegetable oil less than 0.6 (KOH)/(mg/g). Our results showed that Raney Ni produced the oil with AV higher than 1.0 (KOH)/(mg/g) especially at the two hydrogenation stages of 30 min and 90 min. The AVs of hydrogenated oils over all the platinum-catalysts were lower than 1.0 (KOH)/(mg/g). Thus, the sample oil over these platinum-based catalysts showed a better quality and stability towards oxidation and hydrolysis.

Conclusions

The catalytic performance of different platinum supported catalysts (Pt/AC, Pt/MCNTs, Pt/ZrO$_2$ and Pt/TiO$_2$) in the selective hydrogenation of soybean oil was examined. A comparative assessment of the behavior of Pt catalysts and a commercial Raney Ni catalyst was performed. The different synthesized catalysts exhibited diverse characteristics in aspect of particle size, metal dispersion, surface areas, pore size distribution, etc. Meanwhile, all of the platinum based catalysts displayed better activity and higher *cis*-selectivity compared to the commercial Raney Ni catalyst. Among all the investigated catalysts, the Pt/ZrO$_2$ gave rise to the least formation *of trans* isomers and stearic acids at a similar IV and yield a product with required physical and chemical properties. This may be due to the unique pore geometry of the support ZrO$_2$ for Pt catalyst. The above results revealed that the support material had considerable effects on the catalysts characteristics and catalytic behavior during hydrogenation process. Nevertheless, the Pt metal content on the support showed no significant influence on the activity and *cis–trans* selectivity in this trial. It is noteworthy that, under the studied operating conditions, the TFAs concentration is still relatively high for food application, but Pt/ZrO$_2$ is more effective than Raney Ni catalyst to generate biodiesel product and base oils for lubricants with a good stability. Further research is required to optimize the process parameters of the hydrogenation reaction with the Pt catalysts, with the aim to further reducing the formation of the *trans*-isomers.

References

1. Stanković M, Čupić Ž, Gabrovska M, Banković P, Nikolova D, Jovanović D (2015) Characteristics and catalytic behavior of supported NiMgAg/D catalysts in the partial hydrogenation of soybean oil. Reac Kinet Mech Cat 115(1):105–127
2. Chakraborty S, Mandal PK (2015) SPC based on growth models for monitoring the process of hydrogenation of edible oil. J Food Eng 146:192–203
3. Parsania P, Ghavami V, Heydari-Nasab A, Gharachorloo M (2015) The effect of hydrogenation on physical and chemical characteristics of soyabean oil. J Food Biosci Technol 5:87–91
4. Singh D, Rezac ME, Pfromm PH (2009) Partial hydrogenation of soybean oil with minimal trans fat production using a Pt-decorated polymeric membrane reactor. J Am Oil Chem Soc 86(1):93–101
5. Belkacemi K, Boulmerka A, Arul J, Hamoudi S (2006) Hydrogenation of vegetable oils with minimum trans and saturated fatty acid formation over a new generation of Pd-catalyst. Top Catal 37(2):113–120
6. Hark SVD, Härröd M (2001) Fixed-bed hydrogenation at supercritical conditions to form fatty alcohols: the dramatic effects caused by phase transitions in the reactor. Ind Eng Chem Res 40(23):5052–5057
7. Fernandez MB, Tonetto GM, Crapiste GH, Damiani DE (2007) Revisiting the hydrogenation of sunflower oil over a Ni catalyst. J Food Eng 82(2):199–208
8. Cepeda EA, Calvo B (2008) Sunflower oil hydrogenation: study using response surface methodology. J Food Eng 89(4):370–374
9. Plourde Mélanie, Belkacemi Khaled, Arul Joseph (2004) Hydrogenation of sunflower oil with novel Pd catalysts supported on structured silica. Ind Eng Chem Res 43(10):2382–2390

10. Dijkstra AJ (2006) Revisiting the formation of trans isomers during partial hydrogenation of tria-cylglycerol oils. Eur J Lipid Sci Technol 108(3):249–264
11. Willett WC (2012) Dietary fats and coronary heart disease. J Intern Med 272(1):13–24
12. Attia-Skhiri N, Fournier N, Pourci ML, Paul JL (2009) Trans fatty acids: effects on lipoprotein metabolism and cardiovascular risk. Ann Bio Clin 67(5):517–523
13. Philippaerts A, Jacobs PA, Sels BF (2013) Is there still a future for hydrogenated vegetable oils? Angew Chem Int Ed 52(20):5220–5226
14. Micha R, Mozaffarian D (2010) Saturated fat and cardiometabolic risk factors, coronary heart disease, stroke, and diabetes: a fresh look at the evidence. Lipids 45(10):893–905
15. Krstić J, Gabrovska M, Lončarević D, Nikolova D, Radonjić V, Vukelić N, Jovanović DM (2015) Influence of Ni/SiO$_2$ activity on the reaction pathway in sunflower oil hydrogenation. Chem Eng Res Des 100(2):72–80
16. Simonetti S, Martirena M, Ulacco S, Brizuela G (2013) Platinum-nickel catalyst: the effect of promoters in cis-oleic acid adsorption. Appl Surf Sci 264(4):305–311
17. Mcardle S, Girish S, Leahy JJ, Curtin T (2011) Selective hydrogenation of sunflower oil over noble metal catalysts. J Mol Catal A 351(2):179–187
18. Toshtay K, Auyezov AB, Bizhanov ZA, Yeraliyeva AT, Toktasinov SK, Kudaibergen B, Nurakyshev A (2015) Effect of catalyst preparation on the selective hydrogenation of vegetable oil over low percentage Pd/diatomite catalysts. Eurasian Chem Technol J 17:33–39
19. Alshaibani AM (2014) Optimization of Pd-B/γ-Al$_2$O$_3$ catalyst preparation for palm oil hydrogenation by response surface methodology (RSM). Braz J Chem Eng 31(1):69–78
20. Li T, Zhang W, Royzhenhu L, Zhong Q (2009) Nickel-boron alloy catalysts reduce the formation of trans fatty acids in hydrogenated soybean oil. Food Chem 114(2):447–452
21. Cheng HN, Dowd MK, Easson MW, Condon BD (2012) Hydrogenation of cottonseed oil with nickel, palladium and platinum catalysts. J Am Oil Chem Soc 89(8):1557–1566
22. Nohair B, Especel C, Lafaye G, Marécot P, Hoang LC, Barbier J (2005) Palladium supported catalysts for the selective hydrogenation of sunflower oil. J Mol Catal A 229(1–2):117–126
23. Fernández MB, Jhon FSM, Tonetto GM, Damiani DE (2009) Hydrogenation of sunflower oil over different palladium supported catalysts: activity and selectivity. Chem Eng J 155(3):941–949
24. Shao Y, Yin G, Gao Y, Shi P (2006) Durability study of Pt/C and Pt/CNTs catalysts under simulated PEM fuel cell conditions. J Electrochem Soc 153(6):A1093–A1097
25. Esawi AMK, Morsi K, Sayed A, Taher M, Lanka S (2010) Effect of carbon nanotube (CNT) content on the mechanical properties of CNT-reinforced aluminium composites. Compos Sci Technol 70(16):2237–2241
26. Deliy IV, Simakova IL, Ravasio N, Psaro R (2009) Catalytic behaviour of carbon supported platinum group metals in the hydrogenation and isomerization of methyl oleate. Appl Catal A 357(2):170–177
27. Yang M, Yang Y, Nie S, Xie M, Chen F (2012) Analysis and formation of trans fatty acids in corn oil during the heating process. J Am Oil Chem Soc 89(5):859–867
28. Chen Y, Yang Y, Nie S, Yang X, Wang Y, Yang M, Li C, Xie M (2014) The analysis of trans fatty acid profiles in deep frying palm oil and chicken fillets with an improved gas chromatography method. Food Control 44:191–197
29. Brunauer S, Deming LS, Deming WE, Teller E (1940) On a theory of the van der Waals adsorption of gases. J Am Chem Soc 62(7):1723–1732
30. Zhang Y, Zhang HB, Lin GD, Chen P, Yuan YZ, Tsai KR (1999) Preparation, characterization and catalytic hydroformylation properties of carbon nanotubes-supported Rh-phosphine catalyst. Appl Catal A 187(2):213–224
31. Tonetto GM, Jhon FSM, Ferreira ML, Damiani DD (2009) Partial hydrogenation of sunflower oil: use of edible modifiers of the cis/trans -selectivity. J Mol Catal A 299(1–2):88–92
32. McArdle S, Curtin T, Leahy JJ (2010) Hydrogenation of sunflower oil over platinum supported on silica catalysts: preparation, characterisation and catalytic activity. App Catal A 382(2):332–338
33. Iida H, Itoh D, Minowa S, Yanagisawa A, Igarashi A (2015) Hydrogenation of soybean oil over various platinum catalysts: effects of support materials on trans fatty acid levels. Catal Commun 62:1–5
34. Karabulut İ, Kayahan M, Yaprak S (2003) Determination of changes in some physical and chemical properties of soybean oil during hydrogenation. Food Chem 81(3):453–456
35. Karabulut I, Turan S, Ergin G (2004) Effects of chemical interesterification on solid fat content and slip melting point of fat/oil blends. Eur Food Res Technol 218(3):224–229

36. Rao R, Sankar KU, Sambaiah K, Lokesh BR (2001) Differential scanning calorimetric studies on structured lipids from coconut oil triglycerides containing stearic acid. Eur Food Res Technol 212(3):334–343
37. Hmd NL, Sundram K, Siew WL, Aminah A, Mamot S (2002) TAG composition and solid fat content of palm oil, sunflower oil, and palm kernel olein blends before and after chemical interesterification. J Am Oil Chem Soc 79(11):1137–1144
38. Santana A, Fernández X, Larrayoz MA, Recasens F (2008) Vegetable fat hydrogenation in supercritical-fluid solvents: melting behavior analysis by DSC and NMR. J Supercrit Fluids 46(3):322–328